

# The Effect of Stress Biaxiality on Crack Shape Development

Osama A. Terfas

**Abstract**—The development of shape and size of a crack in a pressure vessel under uniaxial and biaxial loadings is important in fitness-for-service evaluations such as leak-before-break. In this work finite element modelling was used to evaluate the mean stress and the J-integral around a front of a surface-breaking crack. A procedure on the basis of ductile tearing resistance curves of high and low constrained fracture mechanics geometries was developed to estimate the amount of ductile crack extension for surface-breaking cracks and to show the evolution of the initial crack shape. The results showed non-uniform constraint levels and crack driving forces around the crack front at large deformation levels. It was also shown that initially semi-elliptical surface cracks under biaxial load developed higher constraint levels around the crack front than in uniaxial tension. However similar crack shapes were observed with more extensions associated with cracks under biaxial loading.

**Keywords**—biaxial load, crack shape, fracture toughness, surface crack, uniaxial load.

## I. INTRODUCTION

THE effect of constraint on three-dimensional cracks encountered in engineering practice is still problematic. The crack shape, size and type of loading all play a substantial role in the failure process. Solutions for ductile crack growth taking account of constraint for surface cracks are not yet available in the literature. The shape of the advancing crack during ductile tearing needs to be understood in flaw evaluation procedures. Similarly it is important to determine the location where the crack growth initiates around the crack front. This identifies the corresponding toughness to be used in defect assessment procedures.

Therefore Part through-wall flaws frequently have to be considered in flaw evaluations, such as fracture or leak-before-break. In such applications it is important to know the evolution of the crack shape with time or deformation. Such predictions have been done in the literature predominantly for the fatigue and stress corrosion cracking modes of failure driven by the stress intensity factor [1]-[5]. Such calculations showed that flaw size, shape and a loading mode effects on the subsequent flaw development. For example, in tension dominated geometries surface flaws tend to acquire a near semi-circular profile until the flaw breaks-through the vessel wall. Conversely under bending dominant loading the flaw evolution is more complex and is a competition between the extension through the thickness and growth on the surface. If allowed to grow, such flaws eventually break-through the vessel wall, leading to leak-before-break or component outage decisions. It is therefore important to predict with confidence the evolution of a crack shape.

Osama A. Terfas, Department of Marine and Offshore Engineering, University of Tripoli, Tripoli, Libya. (phone: 00218-91-3184110; e-mail: osamaterfas@tripoliuniv.edu.ly).

Limited work has been done on the parameters that influence the crack shape under ductile tearing. Reference [6] showed the maximum J-integral occurs near to the free surface and decreased towards the deepest points in deep semi-elliptical surface cracks in tension. Reference [7] studied stress triaxiality and plastic deformation in deep semi-elliptical surface cracks and observed non-uniform values under tension. The crack grows the most at the deepest segment on the crack front and the least at the surface. These observations suggest a non-uniform crack growth under ductile tearing conditions, where a surface flaw may develop through a different pattern of shapes to the final through-wall flaw, compared with the stress intensity factor dominated growth. It is therefore important to be able to predict this flaw evolution pattern for flaw evaluations.

## II. MATERIAL DATA

The material was taken to be isotropic elastic-perfectly plastic ( $n=\infty$ ) with Young's modulus of 200 GPa, Poisson's ratio of 0.49, and a yield strength of 300 MPa. However in general, non-dimensional results are presented. The material followed the von Mises yield criterion and obeyed an associated flow rule. The notation is based on the cylindrical co-ordinate system shown in Fig 1.

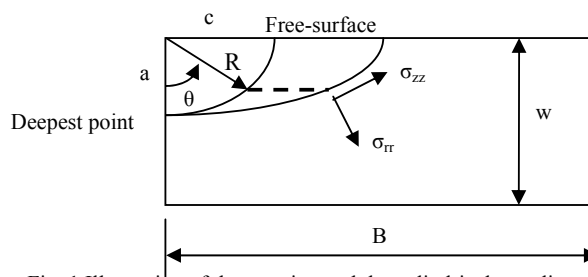


Fig. 1 Illustration of the notation and the cylindrical coordinate system

## III. FINITE ELEMENT MODEL

To capture an accurate stress profile near the crack tip of deep semi-elliptical cracks ( $a/w=0.5$ ,  $a/c=1$ ) a very refined mesh was used close to the crack front. To allow for the correct form of stress singularity at the stationary crack tip under elastic-plastic conditions, collapsed three dimensional continuum hexahedral elements with reduced integration C3D8R with coincident but independent nodes were used.

The average element size was in the range of  $w/1000-2000$  along the crack front, where  $w$  is the plate thickness. The elements were biased towards the free surface to accommodate stress gradients. Due to symmetry only one quarter of the geometry was modelled and symmetry boundary conditions were imposed on the appropriate surfaces as shown in Fig. 2.

The load was applied as displacement boundary conditions, and for biaxial loading the load ratio was defined as  $\beta=(\sigma_x/\sigma_y)_{\text{applied}}=0.5$ . The J-integral was evaluated with domain integral technique adopted in ABAQUS using a contour defined in the far field where J-integral is still path-independent. Thirty concentric rings of elements extended radially from the crack tip. Each ring contained 400 elements: 40 elements along the crack front and 10 around the half circumference. The total number of elements was 107,672. The mesh is shown in Fig. 3.

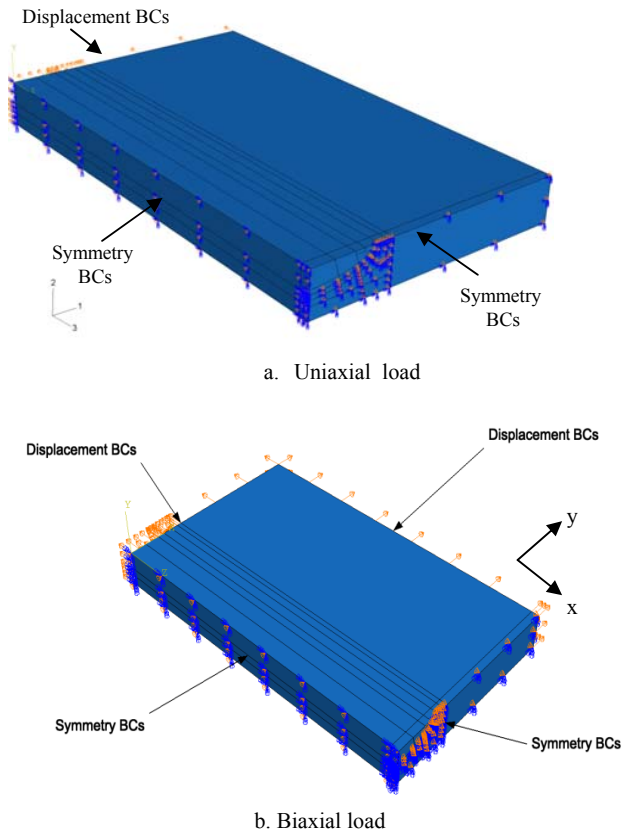


Fig. 2 Quarter model and boundary conditions for elastic-plastic analysis (a) Uniaxial load (b) Biaxial load

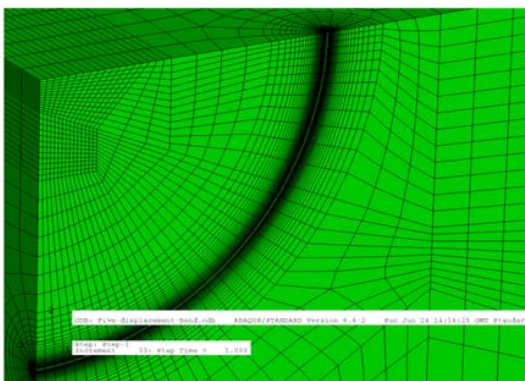


Fig. 3 The mesh for a deep semi-elliptical surface crack

IV. A PROCEDURE TO DETERMINE DUCTILE CRACK EXTENSION

A procedure was developed to determine the ductile crack extension of semi-elliptical surface cracks in flat plates. The method is based on experimental ductile tearing resistance curves obtained from plane strain fracture mechanics specimens with a range of crack tip constraints. The resistance curve  $J-\Delta a$  depends on the mean stress which for plane strain specimens can be expressed as a function of the T-stress. The  $J-\Delta a$  resistance curves in [8] derived from deep and shallow edge cracked bend bars, CTS specimens, centre cracked panels and surface cracked panels shown in Fig. 4 were used as the base data.

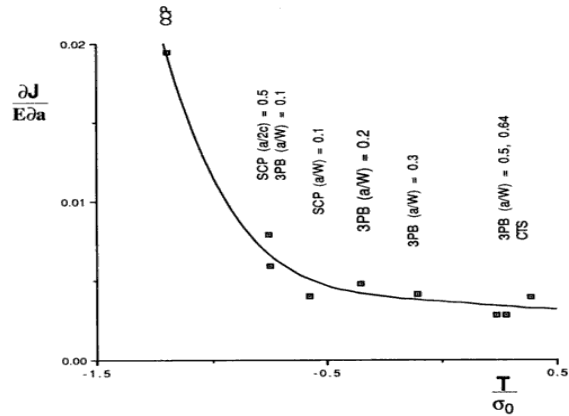


Fig. 4 The slope of the J- $\Delta a$  resistance curve as a function of T [8]

This data was used to derive a relationship between the mean stress which is a function of the T-stress, and the tearing modulus  $T_r = \partial J / \partial \Delta a$ . The mean stress can be simply written as a function of the T-stress:

$$\frac{\sigma_m}{\sigma_0} = 2.39 + \frac{T}{\sigma_0} = 2.39 + Q \tag{1}$$

The term ‘ $T/\sigma_0$ ’ quantifies the level of constraint at the crack tip in a similar way to the Q-parameter [9]-[10]. The tearing modulus  $T_r = (\partial J / (E \delta a))$  derived from Fig. 4 is plotted as a function of the mean stress and is shown in Fig. 5.

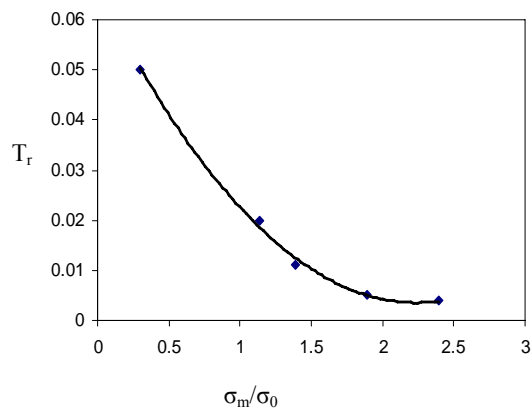


Fig. 5 Tearing modulus as a function of the mean stress

A reduction in the mean stress increases the slope of the  $J$ - $\Delta a$  curve (hence increases the tearing modulus). A curve-fitting procedure gives the relation:

$$T_r = 0.0658 - 0.0557 \left( \frac{\sigma_m}{\sigma_0} \right) + 0.0125 \left( \frac{\sigma_m}{\sigma_0} \right)^2 \quad (2)$$

The tearing modulus is thus taken to be a function of the current level of constraint, but to be independent of deformation level. That is to say the  $J$ - $\Delta a$  curves are taken to be linear. The experimental data in [8] was obtained under plane strain conditions and measured at limited deformation levels, so that constraint is only lost by in-plane effects.

However for surface cracked panels it is clear that constraint can be lost by in-plane effects, by proximity to a free surface, and loss of plane strain conditions as well as effects due to the global bending impinging on the near tip field. It is now assumed that the tearing modulus only depends on the current level of mean stress through (2) for all mechanisms of constraint loss.

The applied  $J$  to cause a defined amount of crack extension  $\Delta a$  can then be written in terms of the tearing modulus which is a function of the mean stress:

$$J = J_{Ic} + \left( \frac{\partial J}{E \partial a} \right) \Delta a \cdot E \quad (3)$$

Here it is convenient to define  $J_{Ic}$  as the applied value of  $J$  corresponding to the initiation of crack extension ( $\Delta a=0$ ). This may be contrasted with the definition used in experimental programmes in which it is convenient to define  $J_{Ic}$  at a small amount of crack extension (i.e.  $\Delta a=0.2\text{mm}$ ). Refer to (3), the crack extension can be in terms of plane strain fracture toughness and the tearing modulus as:

$$\Delta a = \left( \frac{J}{J_{Ic}} - 1 \right) \left/ \left( \frac{T_r \cdot E}{J_{Ic}} \right) \right. \quad J \geq J_{Ic} \quad (4)$$

In order to present non-dimensional results the crack extension is normalised on the smallest uncracked ligament,  $b$ . Equation (4) can then be re-written in a non-dimensional manner:

$$\frac{\Delta a}{b} = (J - J_{Ic}) \cdot \frac{1}{T_r \cdot E \cdot b} \quad \text{For } J \geq J_{Ic} \quad (5)$$

Refer to (5) an estimate of the crack extension around the crack front can be made from a knowledge of  $J_{Ic}$ , the local values of  $J$  and the mean stress (at  $2J/\sigma_0$ ) around the crack front, which defines the tearing modulus  $T_r$ .

To determine the crack shape pattern associated with continued ductile tearing from surface cracks, the initial crack shape was modelled and analysed for the local  $J$ -integral and the mean stress around the crack front.

Although non-dimensional results are presented, the material used was assumed to be isotropic elastic-perfectly plastic with Young's modulus of 200 GPa, Poisson's ratio of 0.49, and a yield strength of 300 MPa.  $J_{Ic}$  was taken to be

$b\sigma_0/100$  so that crack extension occurred in fully plastic conditions. Crack growth was then estimated using (5).

This procedure captures many of the key features of crack extension in surface cracked panels, notably crack extension depends on both the local  $J$  value and the local level of constraint. However in order to capture the effects of finite geometry changes a remeshing procedure was introduced. Following the first estimate of crack extension (defined as step zero) a new crack front was created by extending the original crack front by a small increment using (5). The crack growth increment at the point of the maximum growth on the crack front was chosen for convenience. The crack extensions at the other points around the crack front were scaled to be proportional to the extension at this point. A new finite element mesh was then created for each increment of crack growth and the new crack shape was re-analysed for the mean stress and the  $J$ -integral. As the material response was idealised as perfectly plastic, strain hardening does not raise the flow stress and the applied load changes only as the geometry changes the limit load. As the tearing-resistance curves are linear the increment  $\Delta J$  in each numerical step is related to the increment of local crack extension  $\Delta a$ .

The total value of  $J$  at each point around the crack front represents the sum of the increments of  $J$ :

$$J = \sum \Delta J \quad (6)$$

Similarly, the total crack extension at each point around the crack front is the sum of the increments of crack extension.

$$a = \sum \Delta a \quad (7)$$

This procedure was used to predict the ductile crack extension and crack shape sequences for surface cracks introduced in a large flat plate subject to uniaxial and biaxial tension.

## V. RESULTS

### A. Deep Semi-circular Surface Cracks ( $a/w=0.5$ , $a/c=1$ ) in Uniaxial Tension.

#### 1. Crack Tip Stress Field

Fig. 6 shows the mean stress at a distance  $r=2J/\sigma_0$  along the crack front from the deepest point to the free surface. At low deformation levels ( $b\sigma_0/J=1800$ ), the mean stress was close to the SSY solution over the most of the crack front except at the free surface. This constraint level was low because of in-plane constraint loss (negative T-stress). As plasticity increased the mean stress reduced further. Higher constraint levels occurred in the angular range  $45^\circ$ - $70^\circ$  than at the deepest or surface points.

At the free surface  $\theta = 90^\circ$  the mean stress at low deformation levels was close to the plane stress value. In full plasticity however it approached uni-axial tension (0.3). Fig. 7 shows the non-dimensional  $J$ -integral along the crack front as a function of the parametric angle ( $\theta$ ). The largest  $J$ -values were found at  $45^\circ$ , and  $J$  remained high even at the deepest

point. This contrasts to bending when the J-integral was smaller at the deepest point and attained its largest value at 70° [11].

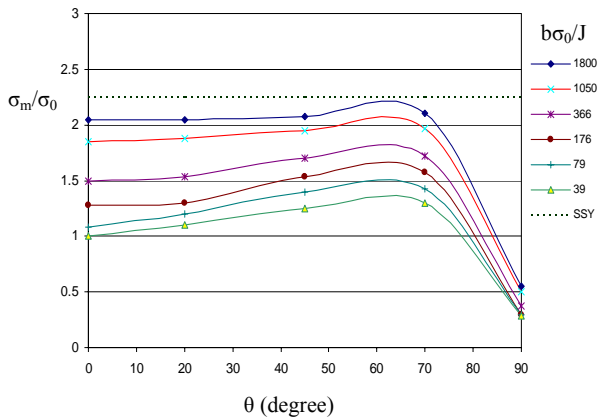


Fig. 6 Mean stress at  $r\sigma_0/J = 2$  as a function of the parametric angle  $\theta$  along the crack front at different levels of deformation for a semi-circular surface crack ( $a/w=0.5, a/c=1$ ) in tension.

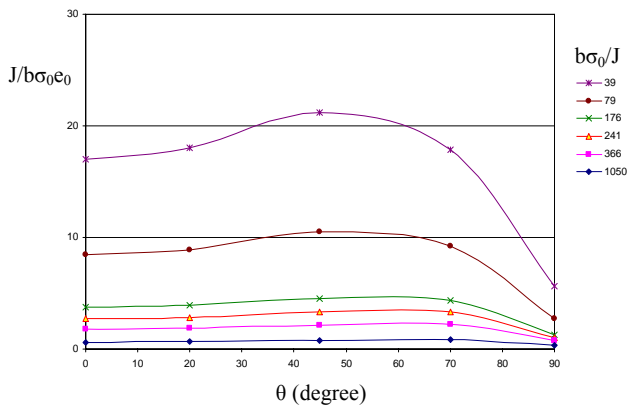


Fig. 7 Non-dimensional J-integral along the crack front in a semi-circular surface crack ( $a/w=0.5, a/c=1$ ) in tension.

**2. Determination of Crack Growth of a Deep Semi-circular Surface Crack in Uniaxial Tension.**

Using the J-integral and mean stress with the procedure described in IV the crack extension was determined. Fig. 8 shows the crack growth  $\Delta a$  as a function of the parametric angle ( $\theta$ ). The crack extended with the highest rate at 45°, combined with growth at the deepest point. To determine the full crack shape sequence three steps were modelled following the procedure described in IV. The results are shown in Fig. 9. The crack grew along the entire crack front with a larger rate at 45°-70° than at the deepest point. Since the level of constraint at high deformation levels was slightly higher at 45°-70° than at the deepest and surface points the maximum crack growth occurred in the range 45°-70°. However the crack continued to grow at the deepest point until it broke through the wall. This contrasts to bending where the crack extended only in the width direction under the surface adopting a boat shape [11].

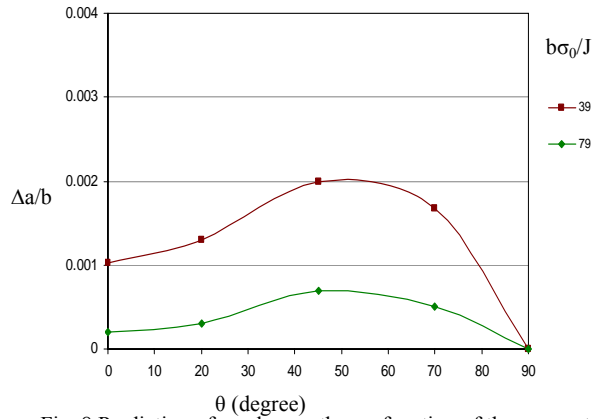


Fig. 8 Prediction of crack growth as a function of the parametric angle ( $\theta$ ) from the deepest point to the free surface in a semi-circular surface crack ( $a/w=0.5, a/c=1$ ) in tension from the initial shape.

The ( $a/c$ ) ratio increased as the crack advances at the deepest point and suppressed at the free surface. This is a different profile to crack shape under fatigue where ( $a/c$ ) becomes constant at approximately one as the crack depth reaches half thickness [12].

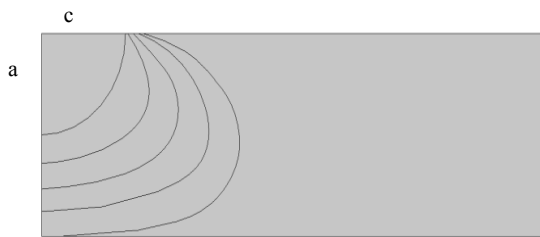


Fig. 9 The crack shape development for a deep semi-circular surface crack ( $a/w=0.5, a/c=1$ ) under ductile tearing in tension.

**B. A deep Semi-elliptical Surface Crack ( $a/w=0.5, a/c=1$ ) Under Biaxial Loading.**

Surface cracks in pressure vessels under internal pressure experience biaxial stress states. Under this condition (biaxiality) the crack may experience and behave in a different manner to uniaxial loading. It is therefore important to investigate the effect of stress biaxiality on the elastic-plastic J-integral, mean stress and the development of ductile tearing.

**1. Crack Tip Stress Field**

Figure (10) shows the mean stress along the crack front as a function of deformation. The maximum mean stress occurred at 70° and reached the plane strain HRR value ( $2.39\sigma_0$ ). The behaviour of mean stress under biaxial loading was different to uniaxial loading where a more uniform mean stress was observed around the crack front. The mean stress at all angles increased significantly under biaxial loading, in contrast to uniaxial loading. Reference [13] shows different results for different biaxial ratio (1:1) when the constraint level at the deepest point in both uniaxial and biaxial loadings was the same.

Fig. 11 shows the non-uniform distribution of the J-integral along the crack front in which the maximum value occurs at 70°. This is should be compared to uniaxial loading where the J-integral distribution was more uniform along the crack front. The maximum crack growth under biaxial loading occurred at 70° where the J-integral and mean stress were maximum as shown in Fig. 12. This can be compared to uniaxial loading where the maximum crack extension was at 45°. Fig. 13 shows the crack growth sequence of a surface crack under biaxial loading.

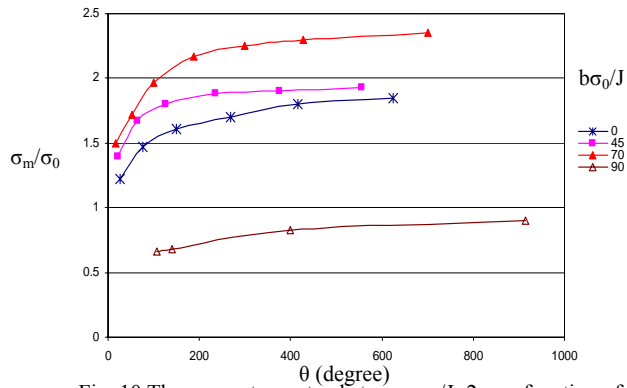


Fig. 10 The mean stress at a distance  $r\sigma_0/J=2$  as a function of deformation level along the crack for a deep semi-circular surface crack in biaxial load ( $a/c=1$ ,  $a/w=0.5$ ).

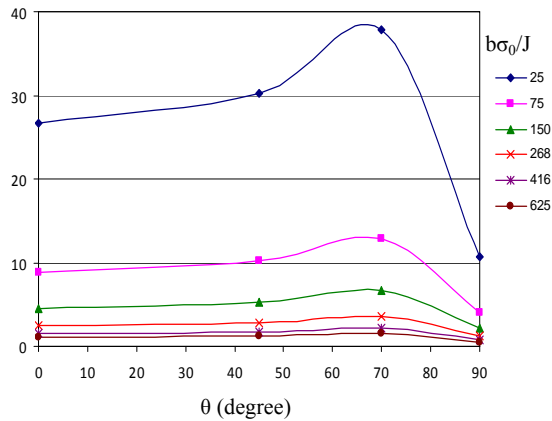


Fig. 11 J-integral along the crack front for a deep semi-circular surface crack in biaxial load,  $a/c=1$ ,  $a/w=0.5$ .

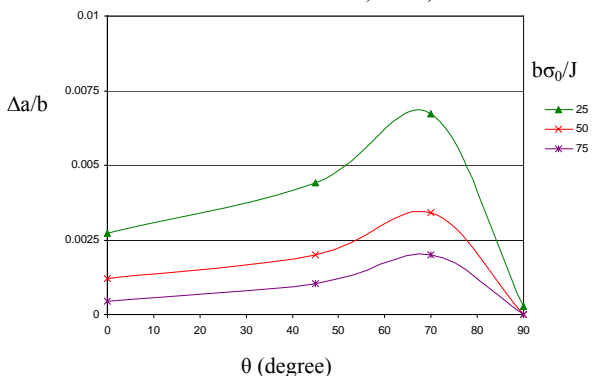


Fig. 12 Crack growth around the crack front as a function of the parametric angle  $\theta$  in a semi-circular surface crack  $a/c=1$ ,  $a/w=0.5$  under biaxial load

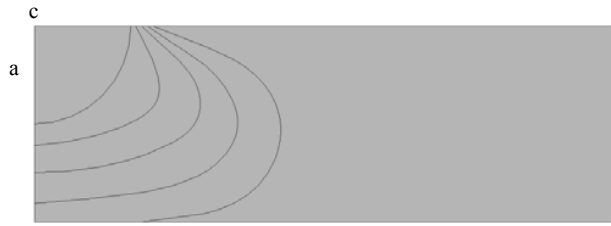


Fig. 13 The crack shape development for a deep semi-circular surface crack ( $a/w=0.5$ ,  $a/c=1$ ) under ductile tearing in biaxial load.

## VI. DISCUSSION

Non uniform crack tip constraint and J-integral distribution along the crack front were observed for surface cracks under tension. The level of constraint along the crack front was close to the SSY solution at low deformation levels ( $b\sigma_0/J > 1500$ ). The low level of mean stress in tension in contained yielding is due to the loss of in-plane constraint ( $T/Q$ ).

As plasticity increased ( $b\sigma_0/J < 300$ ) a further reduction in the mean stress due to an out-of-plane effect was observed. This indicates the use of the standard fracture toughness obtained on deep bend samples for surface cracks assessment is excessively conservative. This is because surface cracks under tension show significant constraint loss near the crack tip, and the margin of safety is expected to increase accordingly.

Deep semi-circular surface cracks ( $a/w=0.5$ ,  $a/c=1$ ) showed a uniform distribution of mean stress and J-integral from the deepest point to 70° at low deformation levels. However as the deformation increased the maximum mean stress appeared at 45°-70°, and the maximum J-integral was at 45°. This trend is consistent with results obtained by [13] for surface cracked geometries with  $a/c=1$  and  $a/w=0.6$  under uniaxial tension. Crack extension was predicted to occur along the entire crack front including the deepest point most notably in the section from 45°-70°. This is also in agreement with [14] where a significant growth was predicted to occur in the circumferential direction of a pipe containing a short surface crack.

However this is slightly different from observation in [7] where the maximum crack growth occurs at the deepest point.

In biaxial loading, the effect of stress biaxiality was significant as higher constraint levels were observed, and a non uniform distribution of the constraint and crack driving force along the crack front was occurred. As a result extensive crack growth occurred in the angular region 45°-70°.

## VII. CONCLUSION

It may be concluded that the mean stress and J-integral were both geometry and load dependent, and both showed a non-uniform behaviour around the crack front at large deformation levels. Both must be taken in to account to make an accurate assessment under ductile tearing conditions. It was noted that single-parameter and two parameter characterisation are not sufficient to describe the stress field at

the crack tip of the surface flaw since the stress triaxiality varies along the crack front which may not coincide with the variation of the J-integral. Non-uniform crack extension around the crack front was observed which was dependent on the type of loading. Under large plastic deformation current investigations showed that the original crack shape was not retained after crack growth by ductile tearing.

The crack was predicted to grow between the deepest point and  $70^\circ$ , hence the crack breaks through the thickness for both uniaxial and biaxial loadings. Similar crack shapes were developed, however a more crack extension in the angular range  $45^\circ$ - $70^\circ$  was occurred under stress biaxiality. The initial crack shape is no longer maintained as the crack advances under elastic-plastic condition.

#### REFERENCES

- [1] L. Hodulak, H. Kordisch, S. Kunzelmann, and E. Sommer, "Influence of the load level on the development of part-through cracks," *International Journal of Fracture*, vol. 14, 1978.
- [2] J. C. JR. Newman, and I. S. Raju. "An empirical stress-intensity factor equation for the surface crack," *Engineering fracture mechanics*, vol. 15, pp. 185-192, 1981.
- [3] A. Carpinteri, "Shape change of surface cracks in round bars under cyclic axial loading," *International Journal of Fatigue*, vol. 15, pp. 21-26, 1993.
- [4] X. B. Lin, and R. A. Smith, "Shape evolution of surface cracks in fatigued round bars with a semicircular circumferential notch," *International Journal of Fatigue*, vol. 21, pp. 965-973, 1999.
- [5] X. B. Lin, and R. A. Smith, "Finite element modelling of fatigue crack growth of surface cracked plates, Part II: Crack shape change," *Engineering Fracture Mechanics*, vol. 63, pp. 523-540, 1999.
- [6] B. Bricksatd, and I. Sattari-Far, "Crack shape development for LBB applications," *Engineering Fracture Mechanics*, vol. 67, pp. 625-646, 2000.
- [7] Y. Chen, and S. Lambert, "Numerical modelling of ductile tearing for semi-elliptical surface cracks in wide plates," *International Journal of Pressure Vessels and Piping*, Vol. 82, pp. 417-426, 2005.
- [8] J. W. Hancock, W. G. Reuter, and D. M. Parks, "Constraint and toughness parameterised by T," "Constraint effect in fracture". ASTM STP 1171. Philadelphia, pp. 21-40, 1993.
- [9] N. P. O'Dowd, and C. F. Shih, "Family of crack-tip fields characterised by a triaxiality parameter-1," Structure of fields. *Journal of Mechanics and Physics of Solids*, vol. 39, pp. 989-1015, 1991.
- [10] N. P. O'Dowd, and C. F. Shih, "Family of crack-tip fields characterised by a triaxiality parameter-2," Fracture applications. *Journal of Mechanics and Physics of Solids*, vol. 40, pp. 939-963, 1992.
- [11] O. Terfas, and B. Bezensek, "The development of a surface crack in a thick vessel under ductile tearing," *Proceedings of 2009 ASME Pressure Vessels and Piping Division Conference*, July 26-30, 2009, Prague Hilton, Czech Republic.
- [12] P. M. Scott, and T. W. Thorpe, "A critical review of crack tip stress intensity factors for semi-elliptic cracks," *Fatigue of Engineering Materials and Structures*, vol. 4, pp. 291-309, 1981.
- [13] X. Wang, "Two-parameter characterization of elastic-plastic crack front fields: Surface cracked plates under tensile loading," *Engineering Fracture Mechanics*, vol. 76, pp. 958-982, 2009.
- [14] E. Berg, B. Skallerud, and C. Thaulow, "Two-parameter fracture mechanics and circumferential crack growth in surface cracked pipelines using line-spring elements," *Engineering Fracture Mechanics*, vol. 75, pp. 17-30, 2008.